IOP Publishing

Letters

Nanotechnology

Nanotechnology **29** (2018) 42LT01 (6pp)

https://doi.org/10.1088/1361-6528/aad671

Letter

Flexible nanograss with highest combination of transparency and haze for optoelectronic plastic substrates

Sajad Haghanifar[1], Rafael T Rodriguez De Vecchis[2], Ki-Joong Kim[3], Jeffrey Wuenschell[3], Sooraj P Sharma[2], Ping Lu[3], Paul Ohodnicki[3] and Paul W Leu[1,2,4]

[1] Department of Industrial Engineering, University of Pittsburgh, Pittsburgh, PA 15261, United States of America
[2] Department of Mechanical Engineering, University of Pittsburgh, Pittsburgh, PA 15261, United States of America
[3] National Energy Technology Laboratory, U.S. Department of Energy, Pittsburgh, PA 15236, United States of America
[4] Department of Chemical Engineering, University of Pittsburgh, PA 15261, United States of America

E-mail: pleu@pitt.edu

Received 5 June 2018, revised 16 July 2018
Accepted for publication 27 July 2018
Published 13 August 2018

Abstract

Transparent polymer substrates have recently received increased attention for various flexible optoelectronic devices. Optoelectronic applications such as solar cells and light emitting-diodes would benefit from substrates with both high transparency and high haze, which increase how much light scatters into or out of the underlying photoactive layers. In this letter, we demonstrate a new flexible nanograss plastic substrate that displays the highest combination of transparency and haze in the literature for polyethylene terephthalate (PET). As opposed to other nanostructures that increase haze at the expense of transparency, our nanograss demonstrates the potential to improve both haze and transparency. Furthermore, the monolithic nanograss may be fabricated in a facile scalable maskless reactive ion etching process without the need for additional lithography or synthesis of nanostructures. Our 9 μm height nanograss sample exhibits a transparency and haze of 92.4% and 89.4%, respectively, and our 34 μm height nanograss displays a transparency and haze of 91.0% and 97.1%, respectively. We also performed durability experiments that demonstrate these nanostructured PET substrates are robust from bending and show similar transmission and haze values after 5000 cycles of bending.

Keywords: light diffuser sheet, sub-wavelength structure, hazy plastic

(Some figures may appear in colour only in the online journal)

Flexible optoelectronics are emerging for a large variety of applications such as flexible versions of traditional rigid displays, smart phones, tablets, and e-paper, as well as new applications such as wearables, RF-ID tags, artificial skin, and the internet of things [1, 2]. Plastics are the most commonly used substrate for flexible optoelectronics due to their high transmittance [3–5]. The optical properties of the substrates are critical for optoelectronic applications as light needs to be coupled into or out of the active region of the device through the transparent substrates. Polyethylene terephthalate (PET), in particular, is often used due to its tolerance to temperature and resistance to solvents as well as high optical transmittance [6]. Various structures have been incorporated into PET substrates for different photon management strategies such as moth-eye-like films [2] and polyurethane acrylate nanostructures [7] for antireflection.

For flexible optoelectronic applications such as organic-light-emitting-diodes [3, 4] and solar cells [5], substrates with both high transmittance and high haze are desirable as increased light scattering results in increased photon outcoupling or incoupling efficiency in these devices, respectively. Plastic-paper hybrids [1], silica nanoparticle arrays [8], and poly(methyl methacrylate)(PMMA)/PET [9, 10] have been demonstrated to increase the amount of light scattering. However, these PET substrates involve lithographic steps and/or the synthesis of nanomaterials that increase cost and complexity for fabrication. These nanostructures tend to increase haze while decreasing transmission as there tends to be tradeoff between these two properties [11]. A combination of both transmission and haze over 90% (at 550 nm wavelength) has yet to be demonstrated in flexible PET substrates.

Recently, we demonstrated nanograss glass substrates that may be fabricated through a scalable maskless, one-step reactive ion etching (RIE) process [12, 13]. In this paper, we demonstrate that a similar maskless RIE process may be utilized to create flexible nanograss PET substrates. These flexible substrates are monolithic and require no additional lithographic processes or synthesis of nanomaterials. These sub-wavelength nanostructures are able to simultaneously provide for antireflection and scattering such that both transparency and haze may be improved. While bare PET has a transparency and haze of 88.4% and 1.1% at 550 nm, respectively, our 9 μm height nanograss samples demonstrate a transparency and haze of 92.4% and 89.4%, respectively. Our 34 μm tall nanograss samples exhibit a transparency and haze of 91.0% and 97.1%, respectively. These nanostructured PET substrates demonstrate the highest combination of transparency and haze at 550 nm of all PET substrates in the literature. Our nanograss samples displays a light scattering angle of 165° compared to 5° for planar PET. We also performed durability experiments that show these nanostructured PET substrates are robust from bending and maintain similar transmission and haze values after 5000 cycles of bending.

Figure 1 shows the results of the fabrication process. Figure 1(a) displays a schematic of the maskless RIE fabrication process (Trion Technology Phantom III). The PET substrate, which is 125 μm thick, is etched by CF_4 and O_2. The etch conditions were optimized to create high-aspect-ratio grass-like nanostructures that maximize both transparency and haze. The CF_4 and O_2 flow rates are 45 and 5 sccm, respectively. The total pressure of the chamber is maintained at 150 mTorr and the power is set at 125 W. During the etching process, CF and CF_2 monomers form polymers that deposit on the PET [14]. These polymers act as a nano-mask that allows for the etching to create high-aspect-ratio nanostructures.

Figure 1(b) shows cross-section SEM image of the nanograss PET. The nanograss shown here was etched for 120 minutes and is about 34 μm in height. The diameter of each nanograss blade is roughly 200–500 nm at the top and gradually decreases to approximately 50–100 nm at the bottom of the structures. Each blade of grass in the texture has a consistent height across the entire substrate. Figure 1(c) shows an overhead view SEM image of the hazy plastic. The distance between adjacent blades is approximately 100–700 nm and uniformly cover the entire substrate. Figure 1(d) plots the height of the nanograss as a function of etch time. The etch rate is approximately constant at about 300 nm min^{-1} based on a linear fit of the various etched samples.

The use of texturing increases the light scattering, thereby creating a PET substrate that exhibits both high haze and high transparency. Additionally, the sub-wavelength dimensions of the nanograss provides for a graduate change in effective index of refraction from the air to the PET substrate that provides for antireflection and thus, increased transparency. A UV–vis–NIR spectrophotometer (PerkinElmer, Lambda 1050) equipped with an 150 mm integrating sphere was used for measuring the total and direct (or specular) transmission of all nanograss PET samples as well as the bare PET. Figure 2 plots the (a) total transmission and (b) haze factor spectra for bare and different height nanograss PET over wavelengths 400–1050 nm. The haze factor is defined as the percent of scattered transmission to the total transmission:

$$H(\lambda) = \left[\frac{\text{scattered transmission}(\lambda)}{\text{total transmission}(\lambda)}\right] \times 100\%, \qquad (1)$$

where λ is the free space wavelength. The direct transmission is all transmitted light that deviates from the incident beam less than or equal to 2.5°, and the scattered transmission is transmitted light that deviates from the incident beam greater than 2.5°. The total transmission is the sum of the direct and scattered transmission. This haze definition follows that given by ASTM D1003 [15]. The nanograss is on the side facing the incident light.

The bare PET has a total transmission of about 88.5% and haze of less than 2.5% across the entire spectrum. The nanograss PET increases both the transmission and haze. For the 9 μm height nanograss PET, the transmission increases to 92.4% and haze to 89.4% at 550 nm wavelength. By increasing the height of nanograss to 18 μm, the transmission improves due to improved antireflection. In this case, the highest transmission of 93.0% is observed. For longer nanograss, the total transmission begins to decrease slightly. The transmission decreases at larger heights due to increased scattered (or diffuse) reflection. In contrast, the haze increases monotonically with increasing height as the scattering probability of the light increases. Beyond 27 μm though, this increase is very minimal.

The haze behavior of the nanograss PET samples can be explained by scalar scattering theory of a single rough surface where the height of the surface has a Gaussian distribution [12, 16, 17]. According to this theory, the wavelength dependent haze at normal angle of incidence is

$$H(\lambda) = \left(1 - \exp\left[-\left(\frac{2\pi\sigma_{rms}[n_1 - n_2(\lambda)]}{\lambda}\right)^2\right]\right) \times 100\%, \qquad (2)$$

where σ_{rms} is the root mean square surface roughness and n_1 and n_2 (λ) are the refractive indices of air and PET,

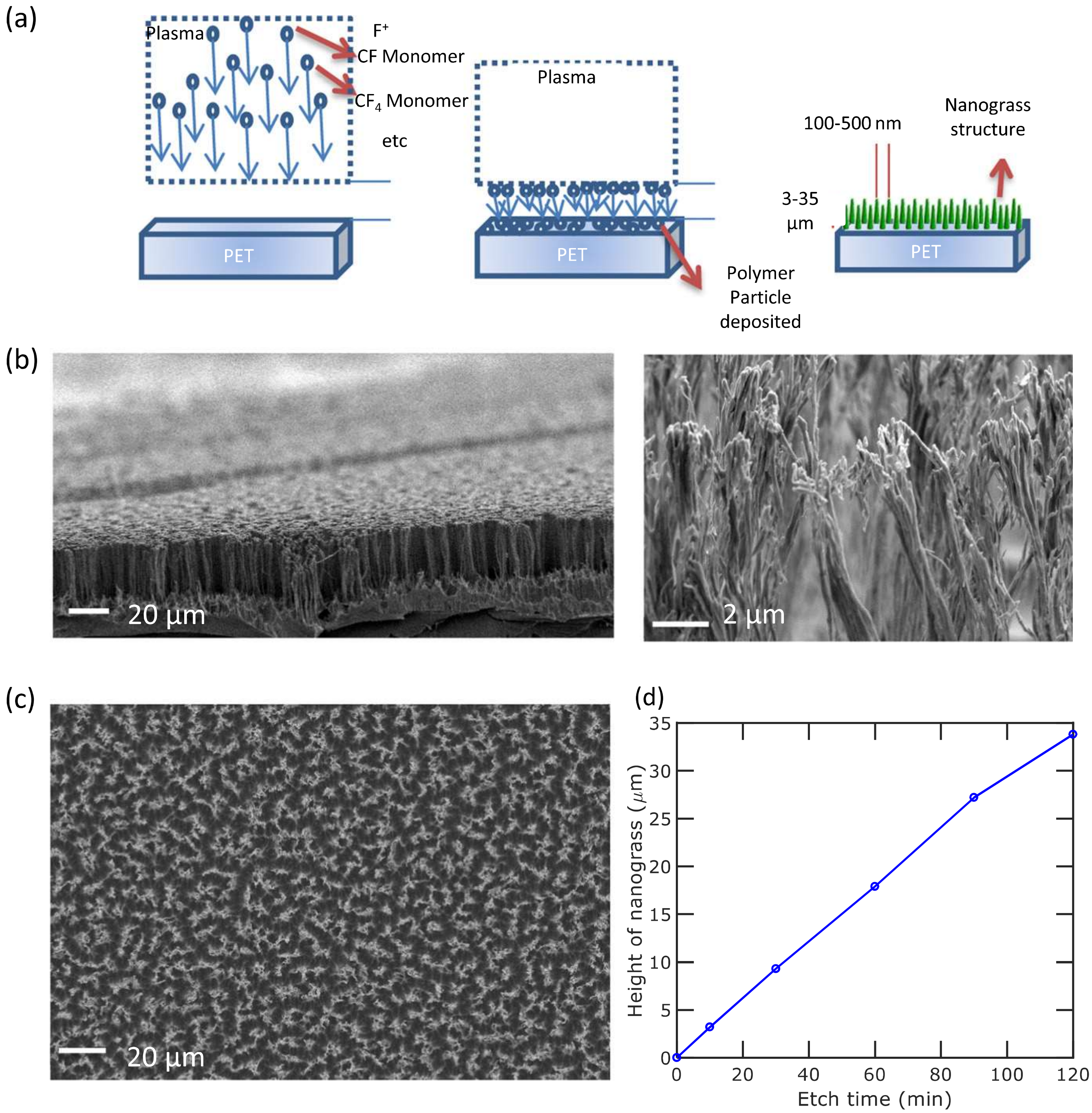

Figure 1. Fabrication of nanograss PET results. (a) Schematic of fabrication process. (b) Cross-section SEM images of 34 μm nanograss PET. (c) Overhead SEM image, and (d) Height of nanograss PET as a function of etch time.

respectively. Figure 2(b) plots our experimental haze results compared to that predicted from equation (2) where σ_{rms} was treated as a fitting parameter. The fits were $\sigma_{rms} = 14$, 68, 290, 410, and 510 nm for the PET with heights of 0, 4, 9, 18, and 34 μm, respectively. The scalar scattering theory results match well with experimental results, though some differences are seen due to lack of considering multiple scattering from the surface in the theory. The haze monotonically increases since the surface roughness also increases with increasing height based on equation (2). This model also shows why the haze decreases with larger wavelengths.

The absorption of a solar cell improves when the path length of scattered light also increases [18]. In order to measure the light scattering ability, we measured the angular distribution function of both bare PET and the 34 μm height nanograss PET as shown in figure 2(c). The scattering angular distribution was measured using a Cary 7000 universal measurement spectrophotometer. In this instrument, incident light is normal to the sample surface with a 5 mm $\times$ 5 mm square beam and the photodetector scans from 10° to 350° ($-10°$); the wavelength scan is from 530 to 570 nm and the wavelength of 550 nm is plotted. The photodetector receives

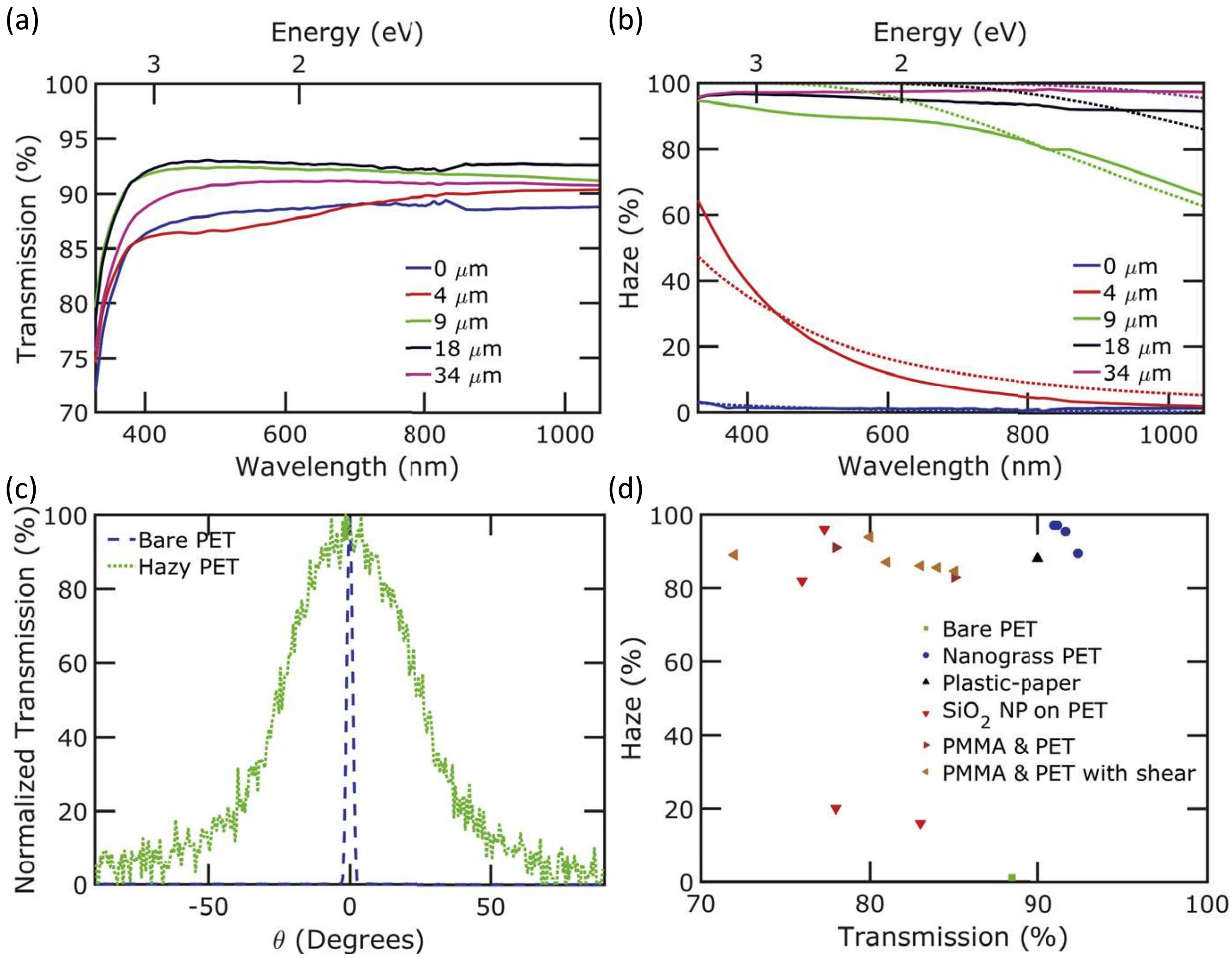

Figure 2. (a) Total transmission and (b) experimental (solid lines) and scalar scattering theory (dashed lines) haze values for smooth and PET with 4, 9, 18, and 34 μm height nanograss. (c) ADF plots of bare PET and nanostructured PET, etched for 120 min. (d) Haze versus transmission for various PET substrates at $\lambda = 550$ nm. Bare PET is shown with a green square and our nanograss PET samples are shown with blue circles. The best data for plastic-paper [1], silica nanoparticle array on PET [8] and doped poly(methyl methacrylate)(PMMA)/poly (ethylene terephthalate) (PET) without [9] and with shear [10] are also shown.

light over a 6° cone and thus, the haze calculated from these plots is not exactly as the same as that measured previously. The scattering angle range is defined as the range of angles in which lights exhibits more than 5% of its highest measured intensity at 0°. As can be seen in figure 2(c), the bare PET has very small scattering angle, 5°, but the 34 μm height nanograss PET has a very large scattering angle of 165°, which shows the light scattering ability of the nanostructured PET.

Figure 2(d) compares the combination of transmission and haze for our nanostructured PET and best high transparency, high haze PET reported in the literature so far, including plastic-paper flexible substrates [1], silica nanoparticle arrays on PET [8], and doped Poly(methyl methacrylate)(PMMA)/poly(ethylene terephthalate) (PET) without [9] and with shear [10]. All data shown in this plot is at a wavelength of 550 nm. Bare PET has a transmission and haze of 88.4 and 1.1%, respectively. The plastic-paper hybrid has a comparable transmission and much higher haze. Most of the other PET samples sacrifice transmission for an increase in haze. In contrast, our nanograss PET exhibits both higher transmission and haze. Our nanograss PET demonstrates the highest combination of transmission and haze of all plastic substrates. The 18 μm height nanograss PET exhibits 93.0% transmission and 95.6% haze and the 34 μm height nanograss PET displays 91.0% transmission and 97.1% haze. In addition, our substrates are the only monolithic samples in the literature. The other PET substrates involve the other materials that need to be synthesized and then introduced into the PET.

Figure 3 plots bending experiment results of our PET. Optical images of both bare PET and 120 min etched nanostructured 34 μm height nanograss PET as the substrates are being bent are shown in figures 3(a) and (b), respectively. The total transmission through the nanograss PET is in fact higher than that of the bare PET due to the antireflection properties of the nanograss. However, the letters through the substrate are completely blurred by the scattering of the light. Figure 3 plots the (c) transmission and (d) haze of the nanograss PET at 550 nm wavelength as a function of bending cycle under tension

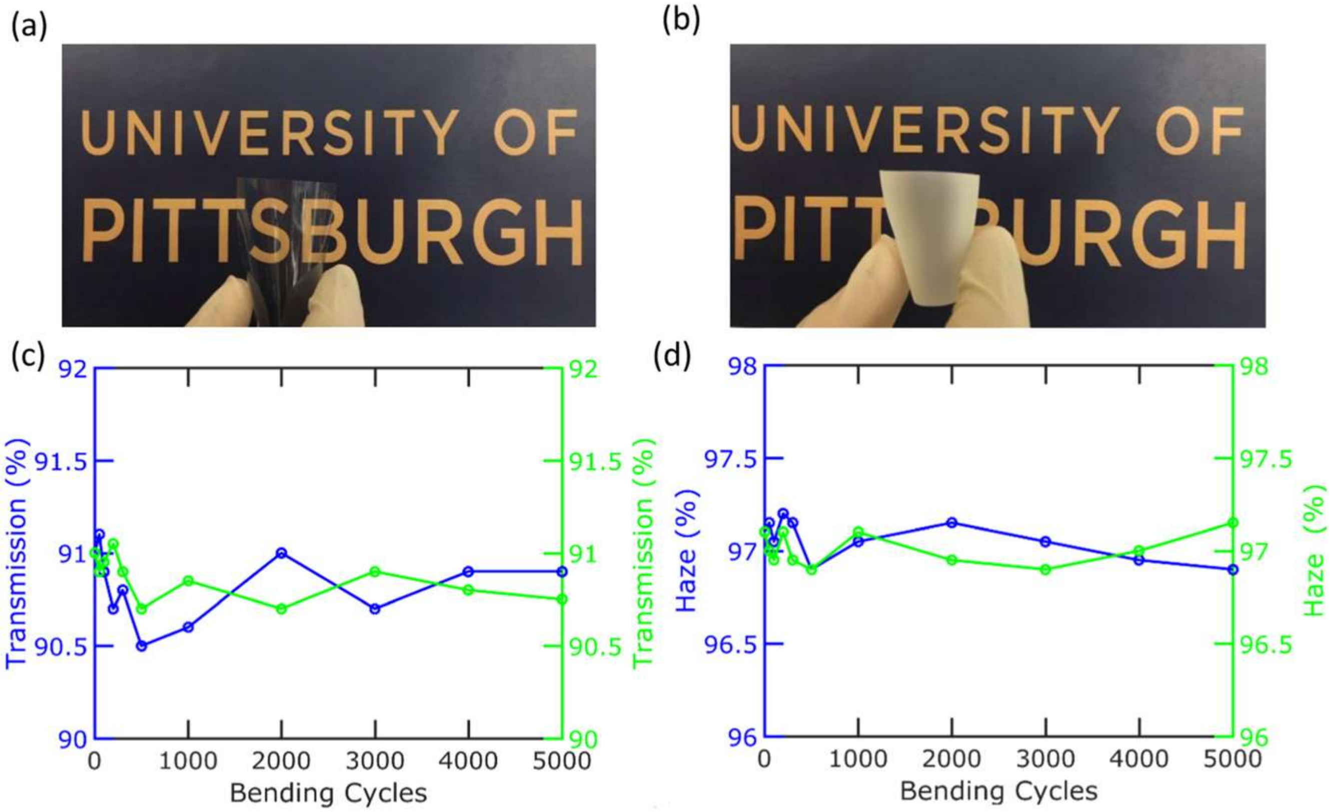

Figure 3. PET bending results. Optical images of (a) bare and (b) 120 min etched nanostructured flexible PET. (c) Transparency and (d) haze at 550 nm as a function of bending cycle, for tension (left y axis) and compression (right y axis).

(left y axis) and compression (right y axis). Bending tests were conducted by bending the 34 μm height nanograss PET substrate around a stainless steel rod with a 1 inch diameter. The thickness of the PET substrate is 125 μm. Two samples with identical size, 3 cm $\times$ 3 cm, were placed under bending compression and tension by bending the etched surface towards and away from the steel rod, respectively. Neither the transmission nor haze are changed significantly after 5000 cycles of bending, for either tension or compression. This suggests that the nanograss PET is robust under bending.

In conclusion, we demonstrate a new nanostructured PET that displays both high transparency and high light scattering ability. The 34 μm height PET showed 91.0% transmission and 97.1% haze at 550 nm wavelength, with 165° scattering angle range. The durability test showed that nanostructured PET substrates are robust from bending and show similar transmission and haze values after 5000 cycles of bending. The combination of flexibility, high transparency and high haze with extra large scattering angle range, makes the nanostructured PET as a strong candidates to use in flexible optoelectronic applications.

Acknowledgments

This work was supported in part by the National Science Foundation (ECCS 1552712).

ORCID iDs

Sajad Haghanifar https://orcid.org/0000-0003-2620-4792
Ki-Joong Kim https://orcid.org/0000-0001-9374-8103
Jeffrey Wuenschell https://orcid.org/0000-0003-2989-8558
Ping Lu https://orcid.org/0000-0002-9201-0956
Paul W Leu https://orcid.org/0000-0002-1599-7144

References

[1] Yao Y *et al* 2016 Light management in plastic–paper hybrid substrate towards high-performance optoelectronics *Energy Environ. Sci.* **9** 2278–85

[2] Tan G, Lee J-H, Lan Y-H, Wei M-K, Peng L-H, Cheng I-C and Wu S-T 2017 Broadband antireflection film with moth-eye-like structure for flexible display applications *Optica* **4** 678–83

[3] Han T-H, Lee Y, Choi M-R, Woo S-H, Bae S-H, Hong B H, Ahn J-H and Lee T-W 2012 Extremely efficient flexible organic light-emitting diodes with modified graphene anode *Nat. Photon.* **6** 105–10

[4] Najafabadi E, Knauer K A, Haske W, Fuentes-Hernandez C and Kippelen B 2012 Highly efficient inverted top-emitting green phosphorescent organic light-emitting diodes on glass and flexible substrates *Appl. Phys. Lett.* **101** 023304

[5] Müller-Meskamp L, Kim Y H, Roch T, Hofmann S, Scholz R, Eckardt S, Leo K and Lasagni A F 2012 Efficiency enhancement of organic solar cells by fabricating periodic

surface textures using direct laser interference patterning *Adv. Mater.* **24** 906–10

[6] Zardetto V, Brown T M, Reale A and Carlo A D 2011 Substrates for flexible electronics: a practical investigation on the electrical, film flexibility, optical, temperature, and solvent resistance properties *J. Polym. Sci.* B **49** 638–48

[7] Zhang J, Shen S, Dong X X and Chen L S 2014 Low-cost fabrication of large area sub-wavelength anti-reflective structures on polymer film using a soft PUA mold *Opt. Express* **22** 1842–51

[8] Yun J, Wang W, Kim S M, Bae T-S, Lee S, Kim D, Lee G-H, Lee H-S and Song M 2015 Light trapping in bendable organic solar cells using silica nanoparticle arrays *Energy Environ. Sci.* **8** 932–40

[9] Liu X, Xiong Y, Shen J and Guo S 2015 Fast fabrication of a novel transparent PMMA light scattering materials with high haze by doping with ordinary polymer *Opt. Express* **23** 17793–804

[10] Liu X, Zhao Z, Xiong Y, Yi P and Guo S 2018 Cost-effective way to improve the optical properties of poly(methyl methacrylate)/poly(ethylene terephthalate) light scattering materials: drop coalescence *Appl. Opt.* **57** 2107–14

[11] Gao T, Haghanifar S, Lindsay M G, Lu P, Kayes M I, Pafchek B D, Zhou Z, Ohodnicki P R and Leu P W 2018 Fundamental performance limits and haze evaluation of metal nanomesh transparent conductors *Adv. Opt. Mater.* **6** 1700829

[12] Haghanifar S, Gao T, Vecchis R T R D, Pafchek B, Jacobs T D B and Leu P W 2017 Ultrahigh-transparency, ultrahigh-haze nanograss glass with fluid-induced switchable haze *Optica* **4** 1522–5

[13] Haghanifar S, Lu P, Kayes M I, Tan S, Kim K-J, Gao T, Ohodnicki P and Leu P W 2018 Self-cleaning, high transmission, near unity haze OTS/silica nanostructured glass *J. Mater. Chem.* C in preparation (https://doi.org/10.1039/C8TC02513D)

[14] Nojiri K 2012 *Dry Etching Technology for Semiconductors* (Berlin: Springer)

[15] ASTM International 2013 D1003-13 Standard Test Method for Haze and Luminous Transmittance of Transparent Plastics https://doi.org/10.1520/D1003-13

[16] Sahraei N, Forberich K, Venkataraj S, Aberle A G and Peters M 2014 Analytical solution for haze values of aluminium-induced texture (AIT) glass superstrates for a-Si:H solar cells *Opt. Express* **22** A53–67

[17] Carniglia C K 1979 Scalar scattering theory for multilayer optical coatings *Opt. Eng.* **18** 182104

[18] Fang Z *et al* 2014 Novel nanostructured paper with ultrahigh transparency and ultrahigh haze for solar cells *Nano Lett.* **14** 765–73